Reaction of Nitric Oxide with Heme Proteins and Model Compounds of Hemoglobin†

Vijay S. Sharma,* T. G. Traylor, and Robert Gardiner

Departments of Medicine and Chemistry, University of California, San Diego, La Jolla, California 92093

H. Mizukami

Department of Biological Sciences, Wayne State University, Detroit, Michigan 48202

Received September 24, 1986; Revised Manuscript Received January 7, 1987

ABSTRACT: Rates for the reaction of nitric oxide with several ferric heme proteins and model compounds have been measured. The NO combination rates are markedly affected by the presence or absence of distal histidine. Elephant myoglobin in which the E7 distal histidine has been replaced by glutamine reacts with NO 500–1000 times faster than do the native hemoglobins or myoglobins. By contrast, there is no difference in the CO combination rate constants of sperm whale and elephant myoglobins. Studies on ferric model compounds for the R and T states of hemoglobin indicate that their NO combination rate constants are similar to those observed for the combination of CO with the corresponding ferro derivatives. The last observation suggests that the presence of an axial water molecule at the ligand binding site of ferric hemoglobin A prevents it from exhibiting significant cooperativity in its reactions with NO.

Of the three gaseous ligands CO, O_2, and NO, the last has the unique distinction of reacting both with the ferrous and ferric hemoglobins. The kinetics of the reactions of NO with ferrous hemoglobin A (Hb A)[1] were studied by Cassoly and Gibson (1975), and the rates of NO dissociation from the nitrosyl derivatives were studied by Moore and Gibson (1976) and Sharma and Ranney (1978). It was observed that the combination reactions of NO with ferrohemoglobin A are fast, are independent of the quaternary structure R or T, show no chain differences, and do not vary with pH or the concentration of organic phosphates. In the studies mentioned above, the dissociation rates were observed to depend markedly on the quaternary structure, pH, concentration of organic phosphates, and the nature of chain, α or β. It was obvious from these studies that the binding of NO to ferro-Hb is very strong—almost irreversible; and the cooperative effects are exhibited only in the dissociation rates. The chain differences are shown most dramatically in the presence of IHP when the proximal histidine to heme bond in α-chains splits, rendering the liganded heme group five-coordinate, without much effecting the β-chains. The lack of variation in the stepwise combination rate constants of NO was explained on the basis of a reaction mechanism in which the ligand first diffuses through the solvent and the protein into the heme pocket, followed by rapid NO to heme bond formation (Morris & Gibson, 1980). It was argued that if NO to heme bond formation is very fast, the combination reaction of NO will become diffusion controlled, showing no dependence on the structural parameters of the protein.

In marked difference to the reactions of NO with ferrohemoglobins, the corresponding reactions of ferric hemoglobins and myoglobins are slow and reversible and show dependence on pH, organic phosphates, and the protein structure (Sharma et al., 1983; Kobayashi et al., 1982). The first studies on ferric Hb^+ A and Mb^+ were made by Keilin and Hartee (1937), who reported that ferric Hb^+ A forms, with nitric oxide, an easily reversible NO-Hb^+ complex. This compound is unstable and soon after its formation changes to a compound that is indistinguishable from NO–ferrous Hb A. On the other hand, the compound formed by the reaction of Mb^+ with NO, Mb^+–NO, is quite stable. Kinetic studies on the reaction of sperm whale ferric Mb with NO yielded combination rate constants of the order of 10^4 M^{-1} s^{-1}, and the results were explained on the basis of fast preequilibrium between the acid and alkaline forms of Mb^+, followed by the rate-determining step in which the water molecule or OH anion at the sixth coordination site is replaced by NO (Kobayashi et al., 1982). Our own ESR and kinetic studies on nitrosyl derivatives of Hb^+ opossum, its α- and β-chains, and sperm whale Mb^+ indicated that the water molecule at the sixth coordination site in ferric heme proteins is stabilized to varying degrees depending on the structure of the heme pocket (Sharma et al., 1983). The α-chains in Hb opossum which lack distal histidine have an NO combination rate constant that is approximately 100 times faster than that for the β-chains. This is particularly interesting as the corresponding CO combination rates in ferro α- and β-chains of Hb opossum are similar to each other as well as to Hb A (Sharma et al., 1982). To investigate this point further, we have studied the reactions of NO with several ferric heme proteins which include α- and β-chains in Hb^+A tetramer, isolated α^+- and β^+-chains of Hb^+A, elephant myoglobin that lacks distal histidine, ferric carp Hb_4, and valency hybrids $\alpha_2^+\beta_2^{CO}$ and $\alpha_2^{CO}\beta_2^+$. In addition we have studied the reactions of two ferric heme model compounds that mimic the behavior of R and T states of hemoglobin in the ferro state. In these model compounds, the stabilization of the axial water molecule by the distal histidine is absent, and

† This work was supported by NIH Grants HL31159 and AM17348.

* Address correspondence to this author at the Department of Medicine, University of California, San Diego.

[1] Abbreviations: Hb A, hemoglobin A; Mb, myoglobin; IHP, inositol hexakis(phosphate); Bistris, 2-[bis(2-hydroxyethyl)amino]-2-(hydroxymethyl)-1,3-propanediol; 2-MI, 2-methylimidazole, a model for the T state of Hb A; chelated protoheme, protohemin–mono-3-(1-imidazolyl)propyl amide monoethyl ester, a model for the R state of Hb A; ESR, electron spin resonance.

0006-2960/87/0426-3837$01.50/0

therefore, the "proximal side effects" are more likely to show up.

Experimental Procedures

Hemolysates of Hb A were prepared by the method of Drabkin. They were oxidized at ice temperature by adding 3 equiv of potassium ferricyanide. The excess of ferricyanide was removed by passing the oxidized hemolysate through Sephadex G-25, equilibrated with 0.1 M Bistris buffer at pH 7.0, and 2,3-diphosphoglycerate (2,3-DPG) was removed by Dintzi's method. α- and β-chains of Hb A were separated by the method of Geraci and Parkhurst (1969). The β-chains were also obtained from the blood of patients with Hb H disease and separated from Hb A as described by Benesch et al. (1964). Sperm whale myoglobin was obtained from Sigma Chemical Co. Elephant heart myoglobin was generously provided by Dr. Mizukami. Valency hybrids, $\alpha_2^{CO}\beta_2^+$ and $\alpha_2^+\beta_2^{CO}$ were obtained by partial oxidation of Hb A with potassium ferricyanide followed by high-performance liquid chromatography on a preparative (carboxymethyl)cellulose column. The gradient used is 0.01 M potassium phosphate buffers of pH 6.8 and 7.5. In 2 h the two hybrids are obtained in good yields and can be used directly for kinetic studies after dialysis against the appropriate buffer. The details of the method are to be published elsewhere (Sharma et al., unpublished results).

Model compounds were dissolved in ethanol containing a drop of dilute sodium hydroxide. Heme concentration was determined by using the published extinction coefficient of 145 $\times 10^3$ for the carboxy form at 408 nm. A calculated volume of the model compound solution was added to ethanol–buffer solvent.

NO and CO gases were obtained from Matheson Gas Products. Saturated solutions of nitric oxide were prepared by bubbling NO for 5 min through deoxygenated 0.1 M Bistris buffer, pH 7.0, in a gas-tight syringe at room temperature. NO was washed through a deoxygenated solution of 1 M NaOH before passing through deoxygenated Bistris buffer. Further dilutions were made by injecting a calculated volume of NO-saturated buffer into deoxygenated buffer also in a gas-tight syringe or, as in the case of model compounds, into deoxygenated Bistris buffer containing desired concentrations of 2-MI and deoxygenated ethanol. For model compounds, most kinetic experiments were made at 20 °C in solutions containing 50% ethanol in 0.1 M Bistris, pH 7.0 (buffer, 50%). Some kinetic experiments were also made in 80% ethanol in 0.1 M Bistris, pH 7.0.

Kinetic experiments were made on a Durrum stopped-flow apparatus with a 2-cm light path cuvette and a tungsten light source. Reactions of ferric β^A-chains were studied by the method of double mixing for reasons described later. In these experiments, ferro β-chains were first mixed with potassium ferricyanide, and after the completion of the oxidation reaction, the oxidized β-chains were then mixed with nitric oxide. Generally, pseudo-first-order conditions were maintained by keeping NO concentration in excess over heme concentration. In a typical kinetic experiment, a small volume of standard solution of ferric heme protein is placed in a gas-tight syringe and nitrogen gas washed with water at room temperature is passed over it for 30 min with frequent gentle rotation of the syringe. A calculated volume of deoxygenated buffer is added to the deoxygenated heme protein. The reaction time course is studied on a stopped-flow spectrophotometer at several NO concentrations. The isosbestic points were determined kinetically by studying the wavelength dependence of the reaction time course (Cassoly & Gibson, 1972).

Table I: Rate Constants for the Combination of Nitric Oxide with Some Ferric Heme Proteins[a]

reaction	isosbestic (nm)	k_{on} (M^{-1} s^{-1})	k_{off} (s^{-1})
$\alpha_2^+\beta_2^+ + NO \rightleftharpoons \alpha_2^{+NO}\beta_2^+$	412	1.71×10^3	0.65
$\alpha_2^+\beta_2^+ + NO \rightleftharpoons \alpha_2^+\beta_2^{+NO}$	413.1	6.4×10^3	1.5
$\beta_4^+ + NO \rightleftharpoons \beta_4^+(NO)_4$	413	13×10^3	3
α^+-chains + $NO \rightleftharpoons \alpha^{+NO}$	411.6	3.3×10^3	2.1
Mb^+ (sperm whale) + NO $\rightleftharpoons Mb^{+NO}$		5.3×10^4	14
Mb^+ (elephant) + NO $\rightleftharpoons Mb^{+NO}$		2.2×10^7	40
Mb (elephant) + CO $\rightleftharpoons$ MbCO		5.6×10^5	
Mb (sperm whale) + CO $\rightleftharpoons$ MbCO		5×10^5	
$\alpha_2^{CO}\beta_2^+ + NO \rightleftharpoons \alpha_2^{CO}\beta_2^{+NO}$		7.3×10^3	1.4
$\alpha_2^+\beta_2^{CO} + NO \rightleftharpoons \alpha_2^{+NO}\beta_2^{CO}$	412.2	1.2×10^3	1.4
Hb^+ carp + NO $\rightleftharpoons$ HB^+–NO carp		5×10^3 (slow phase) 1.4×10^4 (fast phase)	3.2 13

[a] T = 20 °C; 0.1 M Bristris, pH 7.0; all rates measured at 420 nm unless otherwise mentioned.

Table II: Association and Dissociation Constants for the Reaction of NO with Model Compounds[a]

compd	heme concn (after mixing) (μM)	NO concn range (after mixing) (μM)	rate constant
chelated protoheme	0.25–0.5	0.99–50	$k_{on} = (6 \pm 1) \times 10^6$ $k_{off} = 30 \pm 5$
hemin in 2-MI	5.0	3.98–453	$k_{on} = (2 \pm 0.8) \times 10^5$ $k_{off} = 24 \pm 4$

[a] T = 20 °C; all rates measured at 420 nm. Solvent composition, 50% ethanol in 0.1 M Bistris, pH 7.0; [2-MI] = 0.1 M; k_{on} in units of M^{-1} s^{-1} and k_{off} in s^{-1}.

Data Analysis

Pseudo-first-order observed rate constants (k_{obsd}) were obtained from the slopes of ln $(A_\infty - A_t)$ vs. time plots; A_∞ is absorbance when the reaction is complete, and A_t is absorbance at time t. The values of k_{obsd} were then plotted against nitric oxide concentrations to yield the values of k_{on} and k_{off} for the reaction:

$$\text{Hm} + \text{NO} \overset{K}{\rightleftharpoons} \text{Hm–NO}$$

$$K = k_{on}/k_{off} = [\text{Hm–NO}]/[\text{Hm}][\text{NO}] \quad (1)$$

[Hm] and [NO] are concentrations of a model compound or hemoglobin derivative and nitric oxide, respectively. Since NO is in excess:

$$k_{obsd} = k_{on}[\text{NO}]_{tot} + k_{off} \quad (2)$$

The values of NO combination and dissociation rate constants for various ferric hemoglobin derivatives are listed in Table I, and those for the model compounds are listed in Table II. Also listed in Table I are the isosbestic points for the reactions of NO with α^+- and β^+-chains in Hb^+ A tetramer, isolated α^+- and β^+-chains, and the hybrids $\alpha_2^{CO}\beta_2^+$ and $\alpha_2^+\beta_2^{CO}$, as well as the rate constant for the combination of CO with ferro elephant and sperm whale myoglobins.

Results

When a 1911 μM solution of NO is mixed with a 3–5 μM solution of Hb^+ A, the reaction time course is biphasic. The initial pseudo-first-order rate constant is a little more than twice the final rate constant. The ratio of amplitudes (fast phase)/(slow phase) was 0.55. The biphasic nature of the reaction and almost equal proportions of the two phases were also observed at 55 μM Hb^+ A. Similar kinetic runs for ferric

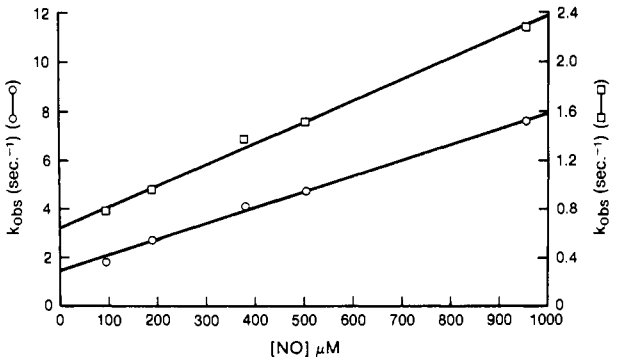

FIGURE 1: k_{obsd} vs. NO concentration plot, in 0.1 M Bistris, pH 7.0. [Hb^+ A] = 5 μM before mixing. (□) α^+-chains in $\alpha_2^+\beta_2^+$; reaction observed at the isosbestic point for the reaction of β-chains (413.1 nm). (○) β^+-chains in $\alpha_2^+\beta_2^+$; reaction observed at the isosbestic point for the reaction of α^+-chains (412 nm).

myoglobin (3 μM) gave a strictly monophasic reaction time course at all NO concentrations.

At 1911 μM NO concentration (before mixing) the reaction was studied at pH 9.2, 7.0, and 6.0. The fraction of the slow phase remained constant at ≈0.5 ± 0.1. On the basis of concentration and pH independence of the relative amplitudes of the two phases and the absence of similar phases in the reactions of ferric myoglobin, the two phases were assigned to the reactions of ferric α- and β-chains in Hb^+ A tetramer. Studies of the wavelength dependence of the reaction time course indicated that the slow phase has an isosbestic point at 412 nm and the fast phase has an isosbestic point at 413.1 nm. Later, on the basis of studies on isolated α^+- and β^+-chains, the slow and fast reactions were assigned to α^+- and β^+-chains in Hb_4 tetramer, respectively. These studies were made at 412 and 413.1 nm for the two phases. The combination and dissociation rate constants obtained from the slope and intercept are listed in Table I. The values of second-order combination rate constants are of the order of 10^3–10^4 and should be compared with the value of (1–5) × 10^4 M^{-1} s^{-1} reported earlier by Kobayashi et al. (1982) for sperm whale Mb^+. It is obvious that β^+-chains combine and dissociate 3–4 times faster than the α^+-chains. In Figure 1 are plotted the values of pseudo-first-order rate constants (k_{obsd}) against NO concentration, and in Figure 2 is shown a pseudo-first-order plot for the biphasic reaction of Hb^+ A with NO.

Reactions of Isolated α^+- and β^+-Chains. Ferric α-chains are stable, and their reactions with NO could be studied without difficulty. The isosbestic point was at 411.6 nm. These reactions were studied at 420 nm at a heme concentration of 4 μM before mixing, and NO concentrations were varied between 973 and 146 μM after mixing. The reactions of ferric β^+-chains were more difficult to study as these chains in the ferric state were unstable and the solutions turned turbid soon after the removal of ferricyanide on Dintzi's column. Out of several preparations, only one yielded ferric β^+-chains that remained stable long enough to allow the study of NO combination reactions. We also observed that if the source of β^+-chains were Hb H isolated by column chromatography from the blood of patients with Hb H disease, the ferric β^+-chains remained stable somewhat longer. In order to study the reactions of β^+-chains in a more reproducible manner, we used the following procedure: Using the double-mixing technique, we first mixed ferro β-chains with a 3–5-fold excess of ferricyanide, and then after the solutions were aged for 4 min, the products of the first mixing were mixed with NO solutions. The two methods gave the same results, except that the double-mixing method can be used reproducibly without

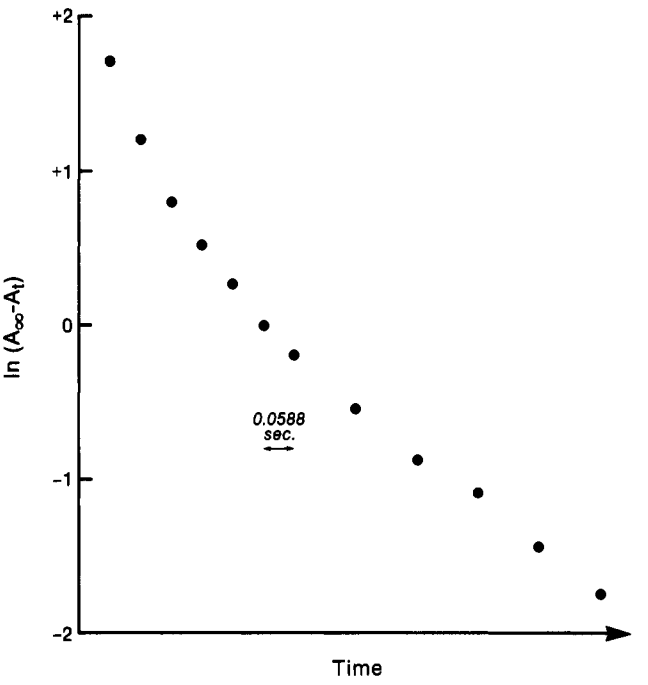

FIGURE 2: Pseudo-first-order kinetic plot for the biphasic reaction of Hb^+ A with nitric oxide. [Hb^+ A] = 2.5 μM after mixing; [NO] = 955.5 μM after mixing. Buffer was 0.1 M Bistris, pH 7.0.

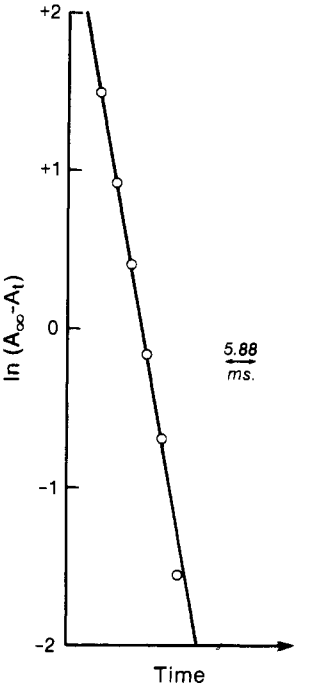

FIGURE 3: Pseudo-first-order kinetic plot for the reaction of NO with ferric Mb elephant. [Mb^+] = 0.4 μM after mixing; [NO] = 7.1 μM after mixing.

worrying about the instability of β^+-chains. The isosbestic point for the β^+-chains was at 413 nm. We have also observed that the reduction reaction of the NO-β^+ complex is considerably faster than that of α^+-chains. However, it does not interfere with the study of NO combination reactions.

Reactions of Elephant Heart Myoglobin. The reactions of elephant heart myoglobin were studied with carbon monoxide as well as with nitric oxide. The reactions of nitric oxide with ferric Mb^+ elephant are very fast. It was, therefore, necessary to use low concentrations of the protein (≈0.4 μM after mixing), and NO concentrations were varied from 2.7 to 12.5 μM. Figure 3 shows a first-order kinetic plot, and in Figure

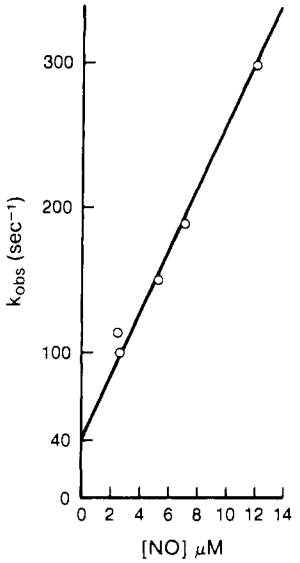

FIGURE 4: k_{obsd} vs. NO concentration plot for Mb^+ elephant, in 0.1 M Bistris, pH 7.0. [Mb^+] = 0.4 μM after mixing.

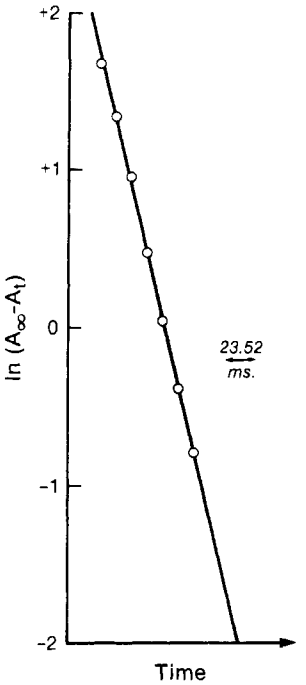

FIGURE 5: Pseudo-first-order kinetic plot for the reaction of ferro-Mb elephant with CO, in 0.1 M Bistris, pH 7.0. [Mb] = 4.0 μM and [CO] = 47.3 μM after mixing.

4 values of k_{obsd} are plotted against NO concentrations. The NO combination rate constant for Mb^+ elephant heart myoglobin, 2.2×10^7 M^{-1} s^{-1}, is approximately 400 times faster than the corresponding reaction for Mb^+ sperm whale and more than 1000 times faster than that of α^+- and β^+-chains of Hb^+ A. The NO dissociation rate constant is about 3 times of the value for Mb^+–NO sperm whale.

Figure 5 shows the first-order kinetic plot for the reaction of CO with ferro Mb elephant. This value of 5.6×10^5 M^{-1} s^{-1} should be compared with the earlier reported value of 5.3×10^5 M^{-1} s^{-1} (Romero-Herrerg et al., 1981) and is not much different than the values reported for horse heart and sperm whale myoglobins (Sharma et al., 1975).

Hb^+ Carp. The reactions of ferric Hb carp with NO were biphasic. The fractions of slow and fast phases were equal at all concentrations of NO. The two phases were assigned to α- and β-chain differences in view of rather well established

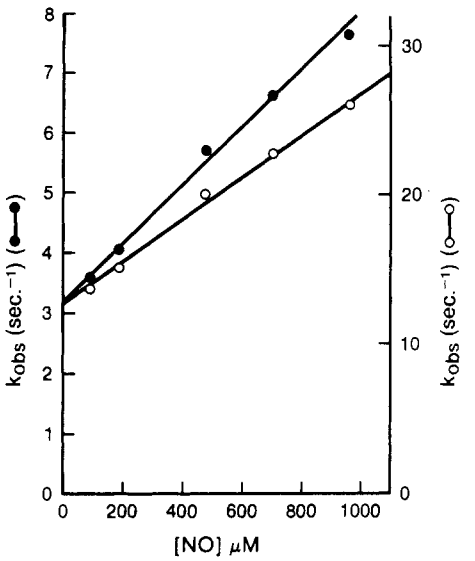

FIGURE 6: k_{obsd} vs. NO concentration plot for the fast (●) and slow (○) phases for Hb^+ carp, in 0.1 M Bistris, pH 7.0. [Hb^+] = 5 μM before mixing.

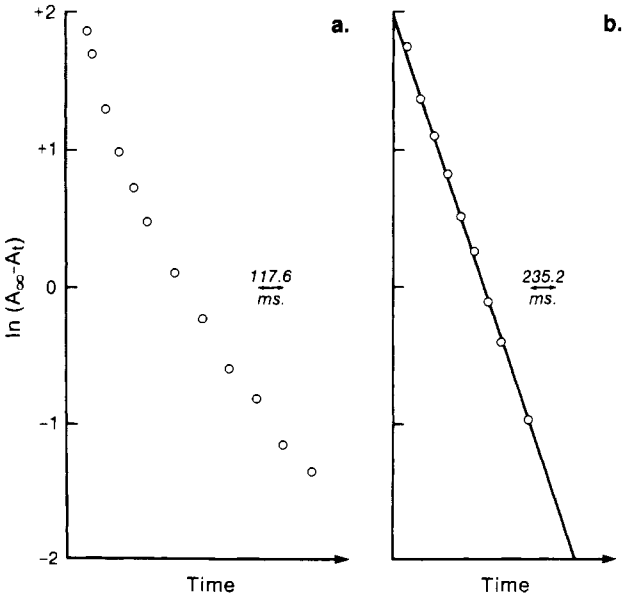

FIGURE 7: Pseudo-first-order kinetic plot for the reactions of NO with $\alpha_2^+\beta_2^{CO}$ and $\alpha_2^{CO}\beta_2^+$. [NO] = 955.5 μM. (a) [$\alpha_2^+\beta_2^{CO}$] = 2.5 μM after mixing. (b) [$\alpha_2^{CO}\beta_2^+$] = 2.5 μM after mixing.

large chain differences in the reactions of ferro Hb carp (Figure 6) (Tan et al., 1973).

Reactions of NO with $\alpha_2^{CO}\beta_2^+$ and $\alpha_2^+\beta_2^{CO}$. Reaction of the hybrid $\alpha_2^{CO}\beta_2^+$ is heterogeneous at pH 8.5, 7.0 (Figure 7a), and 6.0. The initial rates were 3–4 times higher than rates near the end of the reaction. The rates increase as the pH is lowered, and around pH 5.0 the reaction time course becomes monophasic. In Figure 8 the initial rates (k_{obsd}) are plotted against pH. In the alkaline region, the limiting low value of k_{obsd}(initial) has been reached, but the reaction time course is still biphasic. On the acidic side, although the reaction time course has become monophasic, the limiting value is not well-defined and one can only guess that the inflection point is between 5.5 and 6.0. In Figure 9, the values of k_{obsd}(initial) at pH 7.0 are plotted against NO concentrations. The values of NO combination and dissociation rate constants obtained from the slope and intercept in Figure 9 are listed in Table I. These values are very close to the values for ferric β-chains in Hb_4 A, as one would expect.

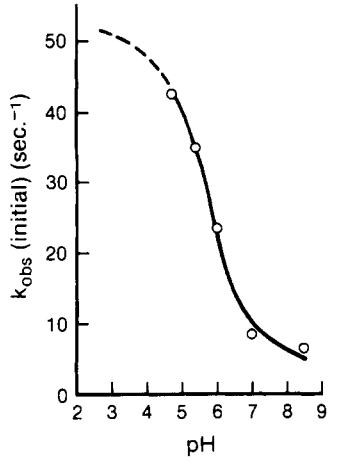

FIGURE 8: Initial k_{obsd} plotted against pH for the reaction of $\alpha_2^{CO}\beta_2^+$ with NO. Other conditions same as in Figure 7b.

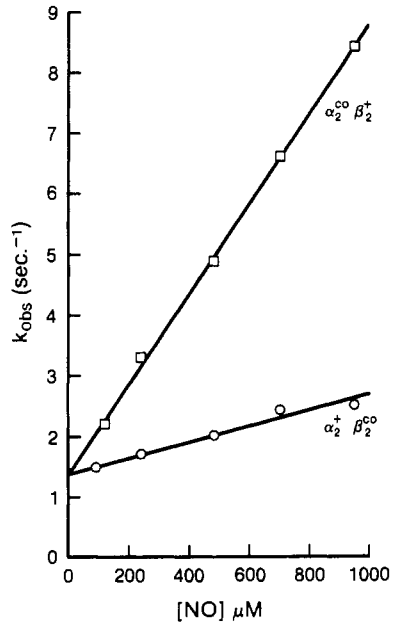

FIGURE 9: k_{obsd} vs. NO concentration plot for $\alpha_2^+\beta_2^{CO}$ and $\alpha_2^{CO}\beta_2^+$, in 0.1 M Bistris, pH 7.0. Concentration on heme basis for both hybrids = 2.5 μM after mixing.

The reaction of ferric subunits in $\alpha_2^+\beta_2^{CO}$ with NO were studied at 420 nm and a total heme concentration of 5 μM before mixing. Nitric oxide concentrations were varied in the range 1911–100 μM before mixing. The reaction time course was strictly monophasic at all NO concentrations. The isosbestic point for the reaction was at 412.2 nm, as compared to 412 nm for α-chains in Hb^+ A and 411.6 nm in isolated α^+-chains. Figure 7b shows a first-order kinetic plot, and in Figure 9 the values of k_{obsd} are plotted against NO concentrations.

Reactions of Ferric Model Compounds with NO. The protohemin–2-methylimidazole complex and chelated protoheme in the ferro state have CO combination and dissociation rate constants similar to those of hemoglobin A in the T and R states, respectively (Traylor et al., 1979). In Table II are listed the experimental conditions, solvent composition, and NO combination and dissociation rate constants for the two model compounds studied. In the case of the 2-MI–hemin complex high concentrations of 2-MI (0.1 M after mixing) were used to exclude the possibility of the reaction proceeding via the four-coordinate free heme. There is a large difference in the first and second binding constants of 2-MI with hemin, and therefore, it can be safely assumed that the main species in this system is the pentacoordinate 2-MI–hemin complex. This point was further checked by making kinetic experiments at a 2-MI concentration of 0.012 M (after mixing). The two sets of experiments gave similar values of NO combination and dissociation rate constants. The effect of solvent composition was studied at two ethanol concentrations: 80% ethanol and 20% Bistris buffer at pH 7.0, and 50% ethanol and 50% Bistris buffer at pH 7.0. While there is not much change in NO dissociation rate constants at 50% and 80% ethanol, the NO combination rate constant at 80% ethanol is a little less than half that at 50% ethanol.

Discussion

Reactions of ferric hemoglobin differ from those of ferrohemoglobin in two important respects. First, these reactions are of quaternary R state as there is very little T-state population in ferric hemoglobin solutions. Second, these are ligand replacement reactions; in the acidic region, the ligand at the sixth coordination site is a water molecule, and in the alkaline region an OH anion occupies the ligand binding site. In sperm whale ferric myoglobin the acid–alkaline pK is 8.3 (Kobayashi et al., 1982). Therefore, it appears that, at pH 7.0, the dominant form of ferric hemoglobin derivative is aquamet. The transition between the two forms is rapid, and rates of H_2O replacement are faster than of OH anion replacement. Therefore, the reactions of NO with ferric hemoglobins are represented by the chemical equations:

$$\text{heme–OH} \underset{-H^+}{\rightleftharpoons} \text{heme}^+\text{–OH}_2 \rightleftharpoons \text{heme}^+ + \text{H}_2\text{O} \quad (3)$$

$$\text{heme}^+ + \text{NO} \rightleftharpoons \text{heme}^+\text{–NO} \quad \text{(rate limiting)} \quad (4)$$

$$\text{sum: } \text{heme}^+\text{–OH}_2 + \text{NO} \rightleftharpoons \text{heme}^+\text{–NO} + \text{H}_2\text{O} \quad (5)$$

The above mechanism is supported by the observation that NO reacts with model compounds and hemoglobins in which the water molecule at the sixth coordination site of heme cannot be stabilized due to the absence of distal histidine at almost the same rates as with ferrohemoglobins (Sharma et al., 1983; Tables I and II). The tertiary structure of the heme pocket, therefore, becomes the most important parameter in determining the reaction rates of ferric hemoglobins with NO.

The data in Table I show that, for all derivatives of Hb^+ A, β^+-chains react faster than α^+-chains. The same trend has been reported for the reactions of CO with deoxy-Hb. The effect is much less clear in the dissociation rate constants, but in this case also, the dissociation rates are generally higher for β^+-chains. Both of these observations are consistent with the presence of E11 Val in β-chains which is believed to overlap with the ligand binding site in the T state (Baldwin & Chothia, 1979). Probably, the R state is not completely free from this effect, and the coordination of water molecules in β^+-chains is weaker.

The most interesting data in Table I is for elephant myoglobin in which the distal E7 His has been replaced by Gln. It reacts with NO 500–1000 times faster than hemoglobins with E7 histidine. At the same time, there is hardly any difference in the CO combination rate constants of sperm whale and elephant myoglobins. A similar observation was made in our earlier study on opossum hemoglobin (HbOP), in which the distal histidine in α-chains has been replaced by glutamine. These α-chains react with NO 100 times faster than β-chains do, without showing any significant difference in the CO combination rate constants of the two chains (Sharma et al., 1983). A similar observation has been reported for aplysia myoglobin. The second-order rate constant for the

reaction of azide with aplysia Mb^+ is 1.5×10^7 M^{-1} s^{-1} as compared to 1.5×10^4 M^{-1} s^{-1} for sperm whale Mb^+, both at pH 6.0 (Giacometti et al., 1981a,b); the CO combination rate constants for the two myoglobins are $(4–6) \times 10^5$ M^{-1} s^{-1} (Wittenberg et al., 1965). As a matter of fact, this is true even for the reactions of oxygen; the presence (Mb horse) or absence (Mb aplysia) of distal histidine makes no difference in the rates of these reactions (Wittenberg et al., 1965). On the basis of these observations, it appears that the high CO combination rates of Hb *Chironomus thummi thummi* and the β-chains of Hb Zurich, both of which also lack the distal histidine, must have some other structural basis [Sharma et al. (1982) and references cited therein]. In the latter case, it should be pointed out that the substitution of E7 His by Arg not only leaves an empty space in the heme pocket but also leaves the entrance to the pocket wide open, which allows ligands easy access to the heme iron (Tucker et al., 1978). The stabilizing effect of distal histidine on the binding of a water molecule in ferric heme derivatives arises out of its ability to form a hydrogen bond with the axial water molecule. Such interactions between the distal histidine and ligand at the sixth coordination site of heme have been proposed by several workers (Makinen et al., 1979; Krishanamoorthi et al., 1984).

Earlier we mentioned that, in the absence of distal histidine, NO combination rates for ferric derivatives are close to those for ferro derivatives. This observation strongly suggests that in these ferric derivatives there is no water molecule at the ligand binding site. This is in disagreement with the NMR results of Krishanamoorthi et al. (1984), which indicate the presence of an axial water molecule in the heme pocket of Mb^+ elephant. The value of 2×10^7 for NO combination rate constants in Mb^+ elephant is too high for a replacement reaction. Perhaps the water molecule observed in NMR studies is not coordinated to the hemin at the ligand binding site. It is interesting to point out that a somewhat similar observation has been made by Benko and Maričić (1978) in NMR studies of Hb^+ glycera and by Giacometti et al. (1981a,b) for aplysia Mb^+, both of which also lack the distal histidine. Furthermore, we have observed that the visible spectrum (700–500 nm) of ferric Mb elephant does not change much between pH 6 and pH 8.5. This strongly indicates the absence of water at the ligand binding site in Mb^+ elephant.

The data on model compounds show in an unambiguous manner that, in the absence of distal histidine to stabilize the water molecule at the sixth coordination site of $heme^+$, the NO combination rates with the R-state model compound (chelated protoheme) are of the same order as those of ferric hemoglobins without distal histidine or of CO, NO, and O_2 with ferrohemoglobins (Sharma et al., 1978).

In their reactions with CO, the 2-MI–heme and chelated protoheme mimic the behavior of the T and R states, respectively, of ferrohemoglobin A (White et al., 1979). The NO combination rate constants of the two model compounds in the ferric state are surprisingly close to the values of the CO combination rate constants for the T and R states of Hb A, indicating that ferric hemoglobin A should exhibit significant cooperativity in its reactions with NO. However, this cooperativity is apparently masked by the presence of an axial water molecule that alters the NO on rates and possibly keeps ferric hemoglobin in the R state. The large difference between the NO combination rate constants of the two model compounds arises from steric hindrance due to the presence of proximal 2-methylimidazole in Fe–NO bond formation.

The hybrid $\alpha_2^{CO}\beta_2^+$ gave a biphasic reaction time course in its reaction with NO. The reaction is monophasic and fast at pH less than 6.0; at pH 8.5 it is 70% slow. In Figure 9 we have plotted the initial observed rate constants for 955 μM NO concentrations against pH. A similar situation was encountered in the reactions of NO with ferric horseradish peroxidase. The two phases were ascribed to the acid and alkaline forms of the protein reacting with NO. The pK for the acid–alkaline transition was around 8.4. For ferric sperm whale myoglobin also this pK is at 8.3 (Kobayashi et al., 1982). In the case of hybrid $\alpha_2^{CO}\beta_2^+$ the pK is 6 or less (Figure 8) and, therefore, cannot be assigned to the acid–alkaline transition. The pK of ≈6 suggests the involvement of a histidine residue in the protein. In fact, a similar reaction involving deprotonation of the proximal histidine (N_ϵ) has been proposed in the reactions of azide with ferric myoglobin of aplysia. The pK of the unliganded ferric Mb aplysia is 5.8 (Giacometti et al., 1981a,b). This value is very close to what we observe in the reactions of NO with the hybrid $\alpha_2^{CO}\beta_2^+$. It is difficult, however, to propose a similar reaction for the hybrid $\alpha_2^{CO}\beta_2^+$ as the equilibria involving such reactions are fast and cannot give rise to a biphasic reaction time course. Furthermore, the Soret absorption peaks for both forms of Mb^+ aplysia were 405 nm or lower. In Figure 10 are shown the difference absorption spectra of $\alpha_2^{CO}\beta_2^+$ at pH 5.4 and 10. The broad peak at pH 5.4 resolved into two components, one absorbing at ≈405 nm and the other at ≈417 nm. At pH 10, the 405-nm peak merges with the 417-nm peak, giving a single symmetrical peak. Subtracting the spectrum at pH 5.4 from that at pH 10.0 revealed a minimum at 405 nm and a maximum at 416.8 nm. This change in the position of the peak at 405 nm suggests replacement of a water molecule at pH 5.4 by a strong-field ligand at pH 10.0, such as imidazole. The two phases in the NO combination reactions at pH 7.0 probably represent the reaction of NO with $\alpha_2^{CO}\beta_2^+$ (H_2O) and $\alpha_2^{CO}\beta_2^+$–Im (E7 His).

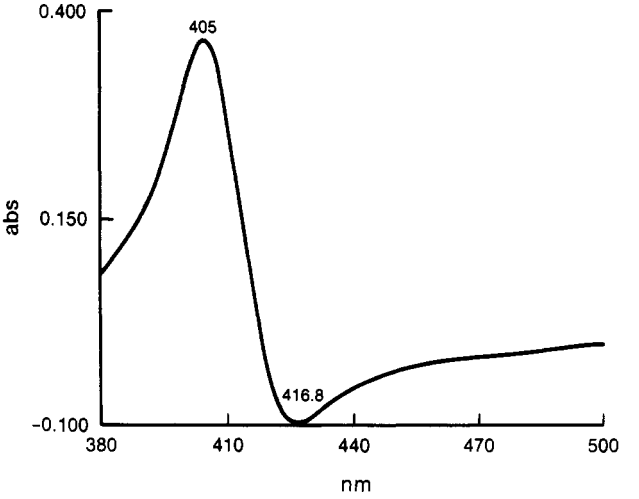

FIGURE 10: Spectrum of $\alpha_2^{CO}\beta_2^+$ at pH 10 minus $\alpha_2^{CO}\beta_2^+$ at pH 5.4.

CONCLUSIONS

In contrast to the ferrohemoproteins that are five-coordinated, the ferric forms can either be five-coordinated or have a water molecule in the sixth position. Therefore, the reaction of NO with the ferric forms can be either a two-step displacement or a simple combination, and this situation dominates the kinetics. It is, therefore, difficult to assess the effects such as steric encumbrance on NO binding to ferric hemoproteins.

The R- and T-state model compounds display the same differences in the reactions of their ferric forms with NO as the corresponding ferro forms toward CO. Thus, ferric hemoglobins should bind NO cooperatively. However, the presence

of a water molecule in the sixth position prevents the cooperativity in a manner that is reminiscent of the displacement of O_2 by CO.

Registry No. Hb^+ A, 12646-21-8; NO, 10102-43-9; CO, 630-08-0; H_2O, 7732-18-5; L-histidine, 71-00-1; chelated protoheme, 108189-62-4; protohemin-2-methylimidazole, 88106-21-2.

References

Baldwin, J., & Chothia, C. (1979) *J. Mol. Biol. 129*, 175–220.

Benesch, R., Gibson, Q. H., & Benesch, R. E. (1964) *J. Biol. Chem. 239*, 1668–1669.

Benko, B., & Maričič, S. (1978) *Croat. Chem. Acta 51*, 369–377.

Cassoly, R., & Gibson, Q. H. (1972) *J. Biol. Chem. 247*, 7332–7341.

Cassoly, R., & Gibson, Q. H. (1975) *J. Mol. Biol. 91*, 301–313.

Geraci, G., Parkhurst, L. J., & Gibson, Q. H. (1969) *J. Biol. Chem. 244*, 4664–4667.

Giacometti, G. M., Ascenzi, P., Bolognesi, M., & Brunori, M. (1981a) *J. Mol. Biol. 146*, 363–374.

Giacometti, G. M., Ascenzi, P., Brunori, M., Rigatti, C., Giacometti, G., & Bolognesi, M. (1981b) *J. Mol. Biol. 151*, 315–319.

Keilin, D., & Hartree, E. F. (1937) *Nature (London) 139*, 548.

Kobayashi, K., Tamura, M., & Hayashi, K. (1982) *Biochemistry 21*, 729–732.

Krishnamoorthi, R., & La Mar, G. N. (1984) *J. Biol. Chem. 259*, 265–270.

Makinen, M. W., Houtchens, R. A., & Caughey, W. S. (1979) *Proc. Natl. Acad. Sci. U.S.A. 76*, 6042–6046.

Moore, E. D., & Gibson, Q. H. (1976) *J. Biol. Chem. 251*, 2788–2794.

Morris, R. J., & Gibson, Q. H. (1980) *J. Biol. Chem. 255*, 8050–8053.

Romero-Herrera, A. E., Goodman, M., Dene, H., Bartnicki, D. E., & Mizukami, H. (1981) *J. Mol. Evol. 17*, 140–147.

Sharma, V. S., & Ranney, H. M. (1978) *J. Biol. Chem. 253*, 6467–6472.

Sharma, V. S., Everse, J., & Ranney, H. M. (1975) *J. Mol. Biol. 95*, 385–393.

Sharma, V. S., Geibel, J. F., & Ranney, H. M. (1978) *Proc. Natl. Acad. Sci. U.S.A. 75*, 3747–3750.

Sharma, V. S., John, M. E., & Waterman, M. R. (1982) *J. Biol. Chem. 257*, 11887–11892.

Tan, A. L., & Noble, R. W. (1973) *J. Biol. Chem. 248*, 2880–2888.

Traylor, T. C., Chang, C. K., Geibel, J., Berzinis, A., Mincey, T., & Cannon, J. (1979) *J. Am. Chem. Soc. 101*, 6716–6731.

Tucker, P. N., Philips, S. E. V., Perutz, M. F., Houtchins, R., & Caughey, W. S. (1978) *Proc. Natl. Acad. Sci. U.S.A. 75*, 1076–1080.

White, D. K., Cannon, J. B., & Traylor, T. G. (1979) *J. Am. Chem. Soc. 101*, 2443–2454.

Wittenberg, B. A., Brunori, M., Antonini, E., Wittenberg, J. B., & Wyman, J. (1965) *Arch. Biochem. Biophys. 111*, 576–579.

Prostatic Growth Factor: Purification and Structural Relationship to Basic Fibroblast Growth Factor†

Michael T. Story,*,‡,§ Joachim Sasse,‖ Stephen C. Jacobs,‡ and Russell K. Lawson‡

Departments of Urology and Biochemistry, Medical College of Wisconsin, Milwaukee, Wisconsin 53226, and Department of Surgery, Harvard Medical School, and The Children's Hospital, Boston, Massachusetts 02115

Received October 30, 1986; Revised Manuscript Received February 6, 1987

ABSTRACT: Prostatic growth factor (PrGF) was purified from alkaline homogenates of human benign prostatic hyperplastic tissue by a combination of ammonium sulfate precipitation, heparin affinity chromatography, and cation-exchange chromatography. The 17 600-dalton, basic (p*I* 10.2) PrGF is related to basic fibroblast growth factor (bFGF) since antisera raised against synthetic peptides with sequence homologies corresponding to an internal peptide and amino- and carboxyl-terminal peptides of bFGF react with the growth factor. The growth factor appears larger than bFGF, suggesting that additional amino-terminal sequences may be present as a result of alkaline extraction in the presence of protease inhibitors.

Jacobs and associates (Jacobs et al., 1979) first reported the presence of a growth-promoting factor in extracts of human tissue prepared from benign prostatic hyperplasia (BPH),[1] well-differentiated prostatic adenocarcinoma (pelvic lymph node), and normal postpubertal prostate. The factor was originally called prostatic osteoblastic factor because it enhanced radiolabeled nucleotide incorporation by cultured fetal rat osteoblasts and calvaria but has also been called prostatic growth factor (PrGF) (Story et al., 1984a; Nishi et al., 1985;

† This work was supported by National Institutes of Health Grant AM31063.

* Address correspondence to this author at the Department of Urology, Medical College of Wisconsin.

‡ Department of Urology, Medical College of Wisconsin.

§ Department of Biochemistry, Medical College of Wisconsin.

‖ Department of Surgery, Harvard Medical School, and The Children's Hospital.

[1] Abbreviations: aFGF, acidic fibroblast growth factor; bFGF, basic fibroblast growth factor; ECGF, endothelial cell growth factor; PrGF, prostatic growth factor; HDGF, hepatoma-derived growth factor; BPH, benign prostatic hyperplasia; NBS, newborn bovine serum; RMA, relative mitogenic activity; ELISA, enzyme-linked immunosorbant assay; CM, carboxymethyl; Tris, tris(hydroxymethyl)aminomethane; TBS, 50 mM Tris with 0.15 M NaCl, pH 7.6; PBS, 0.1 M sodium phosphate with 0.15 M NaCl, pH 7.4; CAPS, 3-(cyclohexylamino)-1-propanesulfonic acid; KLH, keyhole limpet hemocyanin; MHS, *N*-hydroxysuccinimidyl maleimidohexanoate ester; DMF, dimethylformamide; EDTA, ethylenediaminetetraacetic acid disodium salt; SDS-PAGE, sodium dodecyl sulfate–polyacrylamide gel electrophoresis; dpm, disintegrations per minute; TURP, transurethral; kDa, kilodalton(s).

0006-2960/87/0426-3843$01.50/0